*International Journal of Research and Review*
*[Indexed, Peer-Reviewed Journal]*
*Volume 13; Issue: 9; September 2026*
*Website: www.ijrrjournal.com*
*Research Paper* *E-ISSN: 2349-9788; P-ISSN: 2454-2237*

# Blast Fragmentation Prediction and Explosive Selection Using the Kuz-Ram Model: The Case of the Diack Basalt Quarry (Senegal)

**Moumar DIEYE[1], Ablaye THIAM[2], Abdoul Aziz NDIAYE[1], Rokhaya Sall MBAYE[2], Souleye SENE[2]**

[1]École Nationale Supérieure des Mines et de la Géologie (ENSMG), Université Cheikh Anta Diop de Dakar, Dakar, Senegal,
[2]Technical Direction, EPC MINEEX, Dakar, Senegal

Corresponding Author: Moumar DIEYE

**DOI: https://doi.org/10.52403/ijrr.20260914**

## ABSTRACT

This study addresses the prediction of blast fragmentation at the Diack basalt quarry, in the commune of Ngoundiane (Senegal), where basalt is extracted for aggregate production. On site, it was observed that the fragmentation obtained after blasting is not always satisfactory: the presence of oversize boulders often requires the use of a rock-breaker, accelerates crusher wear and increases energy consumption, thereby raising operating costs. The aim of this work was to determine whether the Kuz-Ram model could predict this fragmentation and guide the selection of an explosive better suited to this hard basalt, so as to minimise the occurrence of oversize boulders. To this end, four explosives (ANFO, BLENDEX 70, NITRAM 5 and EXPLUS 90) were compared while keeping exactly the same blast geometry, in order to isolate the effect of the explosive alone. The data used come from laboratory tests on core samples, a structural field survey and the blast records of EPC MINEEX. The rock factor obtained (A = 8.31) confirms that the rock is hard, while the uniformity index (n = 1.29), governed by geometry, indicates a moderately uniform fragmentation. The results show that EXPLUS 90 yields the finest fragmentation (P80 = 486 mm, with only 28.6% of boulders larger than 400 mm) and is the only explosive to simultaneously meet the two industrial requirements set (P80 < 500 mm and oversize at 400 mm < 30%). It was also observed that the charge mass loaded per hole can outweigh the relative weight strength of the explosive. On this basis, an optimal blast pattern, applicable without modifying the existing equipment, is proposed, with the recommendation that it be validated through field measurements.

***Keywords:*** fragmentation; blasting; Kuz-Ram model; basalt; blast pattern; explosive; optimisation.

## 1. INTRODUCTION

In Senegal, the Diack basalt quarry plays an important role in the supply of aggregates for construction works. Drilling and blasting constitute the first stage of the production process. The purpose of a blast is not only to break the rock: it is above all to obtain a fragmentation suited to the crushing plant. This fragmentation quality is referred to as blast fragmentation, and it directly influences the efficiency of the operation.

At Diack, poor fragmentation has been found to cause several difficulties, notably the presence of oversize boulders. This forces the use of a rock-breaker before the primary crusher can be fed, resulting in additional costs, faster equipment wear and higher energy consumption. Comparable difficulties have been reported at other Senegalese quarries subject to blasting (Niane, 2011; Sene, 2011). In this context, it becomes important to better predict the particle size distribution of the material after blasting. Indeed, despite the use of different explosives and several blast patterns, the results obtained do not always meet expectations.

Several empirical models have been developed since the mid-twentieth century to predict fragmentation. Among them, the Kuz-Ram model was selected for this study. It combines three equations: the Kuznetsov (1973) equation, the Cunningham (1983, 1987) uniformity formula, and the Rosin and Rammler (1933) law. It is the most widely used model in practice, first because its input data are readily available in the field, and second because it directly incorporates the relative weight strength of the explosive in its main equation. More recent variants — the KCO model (Ouchterlony and Sanchidrián, 2019), the JKMRC TCM and CZM models (Djordjevic, 1999), the Swebrec function (Ouchterlony, 2005) and the modified Kuz-Ram model (Gheibie et al., 2009) — better represent the fine fraction of the distribution, but they require data or software that were not available for this study.

The research question addressed here is therefore the following: to what extent does the Kuz-Ram model, applied to the geomechanical and structural conditions of the Diack deposit and to the EPC MINEEX blast geometry, allow the prediction of fragmentation and guide the selection of an explosive that optimises productivity? To answer this, four explosives of different strengths (ANFO, BLENDEX 70, NITRAM 5 and EXPLUS 90) are compared on the same geometry: only the explosive changes, which allows its effect to be isolated. The scenarios are then ranked using industrial indicators, and an optimal blast pattern is proposed.

## 2. GEOLOGICAL SETTING OF THE DIACK DEPOSIT

The Diack quarry is located 37 km south-east of Thiès, in the commune of Ngoundiane, east of the Thiès cuesta. It belongs to the western domain of the Senegalo-Mauritanian basin, where meso-cenozoic deposits arranged in a gently west-dipping monocline (Spengler et al., 1966; Ndiaye, 2012) hosted Tertiary volcanism. This volcanism, active from the late Upper Eocene to the Upper Miocene (Bellion and Guiraud, 1984; Cantagrel et al., 1976), resulted from the reactivation of deep north-south faults inherited from the opening of the Atlantic and reactivated during the Eocene (Liger, 1980; Ponsard, 1988; Crevola et al., 1994). Diack constitutes the main outcrop of this volcanism east of the Cap-Vert peninsula (Fig. 1).

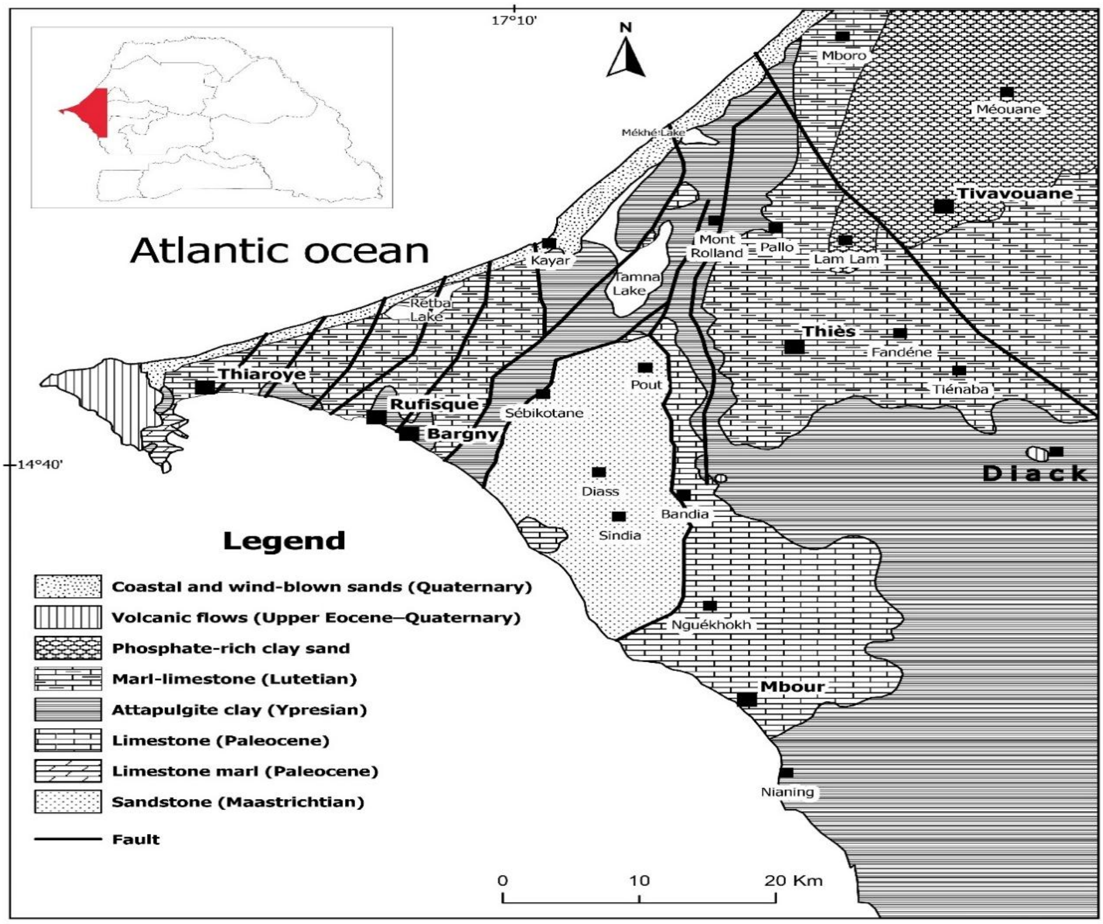


**Fig. 1. Map of Tertiary volcanism of the Cap-Vert peninsula and the Thiès plateau, showing the location of the Diack deposit.**

First reported by Tessier (1952), the deposit corresponds to a basaltic lava lake emplaced within the Ypresian marls and limestones, dated at 10.3 to 7.8 Ma (Crevola et al., 1994; Roger et al., 2009). Beneath about ten metres of ferrallitic weathering, cored boreholes intersect more than 70 m of basalt showing three facies: fine-grained, dominant and consisting mainly of basanites, medium-grained, and coarse-grained (Dia, 1980; Fraudet, 1970). These rock types are distinguished by geometric criteria (grain size, shape, angularity, and roughness) and mechanical properties (hardness and strength), which explain the site's economic appeal for aggregates. Reserves, estimated at 10 million metric tons in 1970, are now being depleted, which makes it all the more important to optimize mining operations (including fragmentation during extraction).

It is this predominance of a very compact fine-grained facies, combined with the polyhedral block pattern inherited from tectonic fracturing, that governs the rock factor A of the Kuz-Ram model and, ultimately, the choice of explosive.

## 3. MATERIALS & METHODS

### 3.1. Rock mass characterisation

Two sources of information were combined to characterise the rock mass. On the one hand, laboratory tests were carried out on core samples collected on site, following standard geomechanical characterisation protocols for rock masses intended for blasting (EPC Groupe, 2014); these provided the uniaxial compressive strength, Young's modulus, density, P-wave velocity and Poisson's ratio. On the other hand, a structural survey was carried out on three benches and presented as a stereographic projection of fracture planes.

These two sources are complementary: laboratory tests describe the strength of the rock matrix, while the structural survey describes the natural block-forming pattern of the rock mass — two aspects that enter separately into the calculation of the rock factor. To position the Diack basalt among materials commonly broken by blasting, the laboratory-measured strength is first related to the Protodiakonov hardness scale (Protodyakonov, 1926), presented in Table 1. This classification, still widely used in open-pit operations, associates each rock category with a hardness coefficient f and a uniaxial compressive strength range; it provides a first qualitative benchmark of blastability before any fragmentation calculation.

**Table 1. Rock classification according to Protodiakonov — hardness scale and uniaxial compressive strength.**

| Category | Coeff. f | Qualification | Rc (kg/cm²) | Rock examples |
|---|---|---|---|---|
| I | 20 | Extremely hard | 2,000 | Hard quartzites, compact basalts |
| II | 15 | Very hard | 1,500 | Hard granites, porphyries, gneiss |
| III | 10 | Hard | 1,000 | Weathered granites, hard limestones, marbles |
| IIIa | 8 | Fairly hard | 800 | Compact limestones, dolomites |
| IV | 6 | Moderately high hardness | 600 | Ordinary sandstones, ferruginous shales |
| IVa | 5 | Medium-high hardness | 500 | Hard clay shales, soft sandstones |
| V | 4 | Medium hardness | 400 | Soft shales, soft limestones |
| Va | 3 | Somewhat soft | 300 | Soft shales, hard marls |
| VI | 2 | Fairly soft | 200 | Hard clays, marls |
| VIa | 1.5 | Soft | 150 | Consistent clays, soft chalks |
| VII | 1 | Very soft | 100 | Loose clays, loams |
| VIIa | 0.8 | Very soft | 80 | Compact sands, gravels |
| VIII | 0.6 | Loose | 60 | Ordinary sands, small gravels |
| IX | 0.5 | Very loose | 50 | Fine sands, silts |
| X | 0.3 | Soluble / flowing | 30 | Waterlogged soils, quicksand, mud |

*f: Protodyakonov hardness coefficient; Rc: uniaxial compressive strength.*

The Protodiakonov scale is, however, not sufficient to feed the Kuz-Ram model. The latter characterises the rock mass through a single rock factor A, which aggregates the nature of the rock mass, the spacing and orientation of discontinuities, and the density and hardness of the rock (Cunningham, 1987). It is therefore to this factor that laboratory measurements and field observations are ultimately reduced. Table 2 presents the classes of A found in the literature and the associated fragmentation behaviour; the value calculated for Diack will be compared against this grid. Its value lies in translating a number into an operational guideline: above A = 7, it is recommended to favour high-energy explosives rather than trying to compensate for the hardness of the rock mass by simply tightening the blast pattern.

**Table 2. Rock mass classification according to the Kuz-Ram rock factor A.**

| Value of A | Classification | Rock mass characteristics | Fragmentation behaviour |
|---|---|---|---|
| $0.8 \leq A < 4$ | Very soft | Weathered, disaggregated or friable rock. Strong fracturing. Low density. | Very easy fragmentation. Risk of excessive fines generation. |
| $4 \leq A < 7$ | Soft to moderately hard | Weakly to moderately cemented sedimentary rock. Moderate to dense fracturing. | Easy fragmentation with conventional explosives (ANFO). Good sensitivity to blast parameters. |
| $7 \leq A < 10$ | Hard | Compact rock (hard limestone, hard sandstone, some basalts). Moderate fracturing. UCS 100–150 MPa. | Demanding fragmentation. High-energy explosives preferred (RWS > 120). Case of the Diack basalt (A = 8.31). |

| | | | |
|---|---|---|---|
| 10 ≤ A < 14 | Very hard | Very resistant massive rock (granite, gabbro, massive basalt). UCS 150–250 MPa. Low fracturing. | Difficult fragmentation. Requires very energetic explosives and a tighter pattern. |
| 14 ≤ A < 21 | Extremely hard | Extremely compact rock (quartzite, unweathered massive granite). UCS > 250 MPa. No exploitable fracturing. | Very difficult fragmentation. Mandatory use of high-density cartridged emulsions. |

*A: rock factor (Cunningham, 1987); UCS: uniaxial compressive strength.*

All the values obtained, both from the core analyses and from the structural survey, are presented and discussed in Section 4.1, where the rock factor A is subsequently calculated from these data.

### 3.2. Explosives compared

Four explosives used on site were compared; they are designated DK1 to DK4. Their technical characteristics are presented in Table 3. They cover a wide range of relative weight strengths (RWS from 100 to 157) and densities, making them a relevant panel for comparison.

**Table 3. Technical characteristics of the four explosives compared.**

| **Parameter** | **DK1 (ANFO)** | **DK2 (BLENDEX 70)** | **DK3 (NITRAM 5)** | **DK4 (EXPLUS 90)** |
|---|---|---|---|---|
| Density (kg/m³) | 800 | 1,200 | 1,200 | 1,200 |
| Specific energy (MJ/kg) | 3.0 | 3.0 | 3.6 | 4.7 |
| RWS (%) | 100 | 100 | 120 | 157 |
| VOD (m/s) | 3,500 | 4,700 | 5,500 | 5,500 |
| Detonation pressure (GPa) | 7 | 14 | 17 | 17 |
| Charge per hole (kg) | 71.91 | 107.86 | 81.85 | 81.85 |

*RWS: Relative Weight Strength relative to ANFO (reference = 100); VOD: Velocity of Detonation; DK1–DK4: designation of the experimental blast scenarios.*

### 3.3. Blast geometry

The blast geometry, identical for all four scenarios, is summarised in Table 4. This is essential to the approach: since only the explosive changes from one case to another, the differences observed in fragmentation stem from the explosive and not from the geometry. The rock volume and mass per hole thus remain constant (168 m³ and 495.4 t).

**Table 4. Geometric parameters of the blast pattern (common to the four scenarios).**

| **Parameter** | **Symbol** | **Value** | **Unit** |
|---|---|---|---|
| Bench height | *H* | 12.0 | m |
| Burden | *B* | 3.5 | m |
| Spacing | *Es* | 4.0 | m |
| Hole diameter | *D* | 102 | mm |
| Stemming length | *Lb* | 1.5 | m |
| Hole length | *Lf* | 12.5 | m |
| Subdrilling | — | 0.5 | m |
| Hole inclination | — | 90° | vertical |

*Lf = H + subdrilling.*

### 3.4. The Kuz-Ram model

The Kuz-Ram model is an empirical model that directly relates the fragmentation obtained to blast parameters, through formulae established from field trials and observations. Its name comes from its two main components: Kuz for Kuznetsov (1973), who proposed the formula giving the mean fragment size from the volume of rock broken and the explosive charge, and Ram for Rosin and Rammler (1933), whose law is used to plot the particle size distribution curve.

Cunningham (1983, 1987) completed the model by introducing the relative weight strength of the explosive (RWS) and a formula giving the uniformity index n.
The model thus rests on three linked equations. The first calculates the median fragment size X50, i.e. the size below which half of the broken muck pile passes; it depends on the rock factor A, the volume broken per hole, the charge, and the RWS of the explosive. The second gives the uniformity index n, which describes the shape of the curve: a high n reflects fragments of homogeneous size, while a low n indicates strong dispersion. This index depends only on the blast geometry (burden, spacing, diameter, stemming, drilling accuracy). The third, the Rosin-Rammler law, combines X50 and n to plot the complete particle size distribution curve, from which the indicators used in the quarry are extracted: P80, P99 and the oversize rate. This structure is what makes the model suited to the present case: all the data it requires were available at Diack, and RWS appears directly in its main equation, which allows four explosives to be compared at constant geometry.
The first equation, due to Kuznetsov (1973), gives the median fragment size:

$$X_{50} = A\left(\frac{V_0}{Q}\right)^{0.8} Q^{\frac{1}{6}} \left(\frac{E}{115}\right)^{-\frac{19}{30}} \tag{1}$$

where A is the rock factor, V0 the volume of rock broken per hole (m³), Q the charge per hole (kg), and E the relative weight strength of the explosive (RWS, in % of ANFO).

The second equation, due to Cunningham (1987), gives the uniformity index n:

$$n = \left(2.2 - 14\frac{B}{D}\right)\left(1 - \frac{\sigma_f}{B}\right)\sqrt{\left(\frac{1+S/B}{2}\right)\left(0.1 + \left|\frac{L_{cp} - L_{cc}}{L}\right|\right)^{0.1}\left(\frac{L}{H}\right)} \tag{2}$$

where B is the burden (m), S the spacing (m), D the hole diameter (mm), σf the standard deviation of drilling accuracy (m), Lcp the bottom charge length (m), Lcc the column charge length (m), H the bench height (m), and L the total charge length (m).
The third equation, the Rosin and Rammler (1933) law, is finally used to plot the complete particle size distribution curve:

$$P(x) = 100\left[1 - \exp\left(-\ln 2\left(\frac{X}{X_{50}}\right)^{n}\right)\right] \tag{3}$$

where P(x) is the percentage of fragments passing size x.
The rock factor is calculated from A = 0.06 × (RMD + JPS + JPA + RDI + HF), where RMD describes the rock mass, JPS the joint spacing, JPA their orientation, RDI = 25ρ − 50 the density influence, and HF = E/3 the hardness factor (Cunningham, 1987).
The work was carried out in five steps. Data were first collected; the choice of the Kuz-Ram model was then justified; the three parameters (A, n and X50) were calculated for each scenario; it was then verified, using performance indicators (S/B, H/B, powder factor, normalised stemming length, drilling accuracy), that the geometry fell within the ranges recommended in the literature (EPC Groupe, 2017); finally, the four scenarios were compared through the Rosin-Rammler curves to derive an optimal blast pattern.

## 4. RESULT AND DISCUSSION

### 4.1. Rock mass characteristics

Rock mass characterisation is the starting point for applying the model, since it sets the rock factor A. The laboratory tests on core samples collected on site and the structural survey carried out on three benches provided the mechanical and structural parameters required for the calculation. The main results are summarised in Table 5.

**Table 5. Geomechanical and structural parameters of the Diack basalt.**

| Parameter | Unit | Value | Source |
|---|---|---|---|
| Density (ρ) | t/m³ | 2.95 | Laboratory |
| Uniaxial compressive strength (UCS) | MPa | 138 | Laboratory |
| Young's modulus (E) | GPa | 44 | Laboratory |
| P-wave velocity (Vp) | m/s | 4,250 | Laboratory |
| Poisson's ratio (ν) | — | 0.25 | Laboratory |
| Fracture spacing (JPS) | cm | 10 (oversize) | Field |
| Joint orientation (JPA) | — | Normal strike | Field |

*JPS: Joint Plane Spacing; JPA: Joint Plane Angle, orientation of joints relative to the blast direction.*

These values reflect a massive, very compact basalt, classified among hard rocks (Table 1) and therefore difficult to fragment. The structural survey nonetheless shows that the rock mass is fractured: two quasi-conjugate, gently dipping discontinuity families are identified, oriented north-east and south-east (Fig. 2 and 3), which break the rock into polyhedral blocks. Fragmentation therefore depends both on the hardness of the rock and on its degree of fracturing.

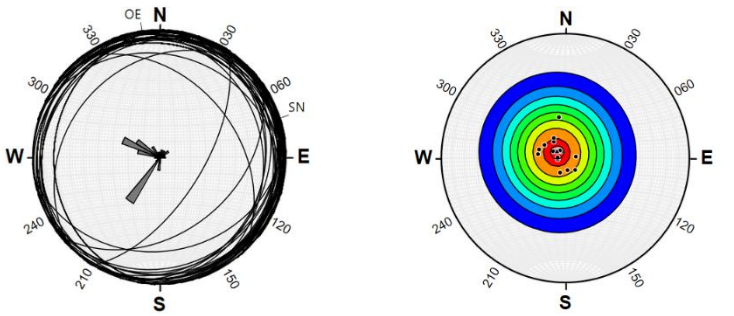


**Fig. 2. Stereographic projection of fracture planes recorded on the benches of the Diack quarry: (A) fracture planes; (B) pole density of the planes.**

**Fig.3: Fracture planes that divide the massif into a polyhedral block**

### 4.2. Rock factor and uniformity index

Adding the five components (RMD = 50; JPS = 20; JPA = 30; RDI = 23.73; HF = 14.79) gives a rock factor A = 8.31, identical for all four scenarios since the rock does not change. On the Kuz-Ram scale (Table 2), this value places the Diack basalt among hard rocks, consistent with the laboratory measurements. An important point emerges: fragmentation will depend almost exclusively on the energy delivered by the explosive.

The Cunningham (1987) formula gives a uniformity index n = 1.29 (Eq. 2), also common to all scenarios since it is governed by geometry rather than by the explosive. According to the Cunningham (1987) scale, this value reflects a moderately uniform distribution. This result is not ideal but remains acceptable. It mainly means that the uniformity index n cannot be improved by simply changing the explosive: this would require modifying the geometry itself.

### 4.3. Median size and particle size distribution

The median size X50 (Eq. 1), which depends on both the charge per hole and the RWS, is what differentiates the scenarios. The main indicators extracted from the Rosin-Rammler curves (Eq. 3; Fig. 4) are summarised in Table 6, which also incorporates the energetic parameters and a relative economic evaluation to facilitate the overall comparison of the four scenarios.

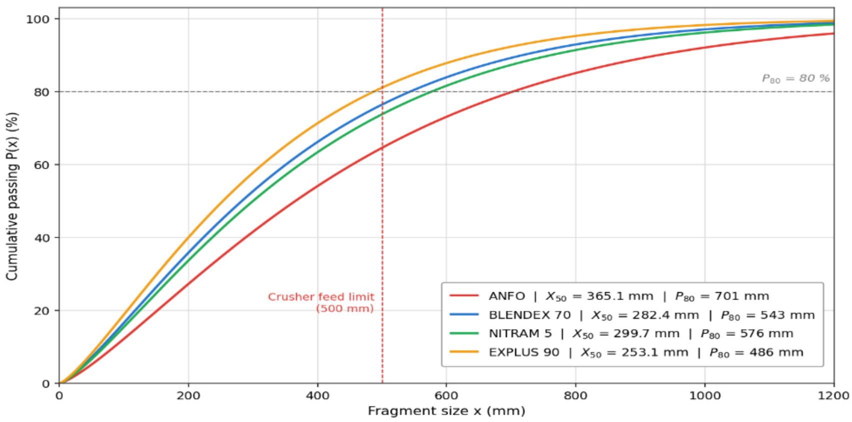


**Fig. 4. Particle size distribution curves predicted by the Kuz-Ram model (Rosin-Rammler law) for the four scenarios.**

**Table 6. Summary of the energetic parameters, particle size indicators and multi-criteria ranking of the four scenarios.**

| **Indicator** | **DK1 (ANFO)** | **DK2 (BLENDEX 70)** | **DK3 (NITRAM 5)** | **DK4 (EXPLUS 90)** |
|---|---|---|---|---|
| **Energetic parameters** | | | | |
| RWS (%) | 100 | 100 | 120 | 157 |
| Charge per hole (kg) | 71.91 | 107.86 | 81.85 | 81.85 |
| Energy per hole (MJ) | 215.72 | 323.58 | 294.64 | 384.67 |
| **Fragmentation results** | | | | |
| X50 (mm) | **365.1** | **282.4** | **299.7** | **253.1** |
| P80 (mm) | **701.0** | **542.2** | **575.4** | **486.1** |
| P99 (mm) | **1,582** | **1,224** | **1,299** | **1,097** |
| Boulders > 300 mm (%) | **58.4** | **47.3** | **50.0** | **42.2** |
| Boulders > 400 mm (%) | **45.8** | **33.7** | **36.6** | **28.6** |
| **Economic evaluation and ranking** | | | | |
| Relative purchase cost | Low | Medium | High | **Very high** |
| Overall ranking | 4th | 2nd | 3rd | **1st** |

*X50: median fragmentation diameter; P80, P99: diameters corresponding to the 80th and 99th percentiles of the particle size distribution. Ranking is established in increasing order of X50, a lower value indicating better fragmentation; purchase cost is assessed on a relative basis using unit explosive prices.*

The ranking is clear-cut: the EXPLUS 90 curve is consistently the finest, while the ANFO curve is the coarsest; BLENDEX 70 and NITRAM 5 fall in between. This ranking is explained by the combination of charge per hole and relative weight strength of the explosive. ANFO proves clearly unsuited to the Diack basalt: its low density (800 kg/m³) limits the charge to 71.91 kg per hole, and its detonation velocity (3,500 m/s), lower than the wave velocity in the rock (4,250 m/s), results in poor energy coupling, hence the coarsest fragmentation of the panel (X50 = 365 mm, P80 = 701 mm).

BLENDEX 70 illustrates, conversely, the role of the charge mass: at an identical RWS (100), its density of 1,200 kg/m³ allows 107.86 kg to be loaded per hole and lowers P80 to 542 mm, a gain of 23%. The comparison with NITRAM 5 is in this respect the most striking result of the study: although it has a higher RWS (120), a faster VOD and a higher detonation pressure, it lags behind (P80 = 575 mm) because its charge per hole is lower (81.85 kg).

In the Kuznetsov formula, the absolute charge Q can therefore sometimes outweigh the relative strength, a finding already reported on other hard rock masses (Sene, 2011; Houssam, 2020). EXPLUS 90 ultimately stands out as the best choice: the only explosive combining a very high RWS (157), a VOD exceeding the wave velocity in the rock (5,500 m/s) and a maximum detonation pressure (17 GPa), it outperforms all indicators (X50 = 253 mm, P80 = 486 mm, 28.6% of boulders larger than 400 mm) and is the only one to cross both industrial thresholds set, a P80 below 500 mm and an oversize rate below 30%.

These differences define the available levers for action. At Diack, the rock factor A is fixed by the deposit and the geometry is fixed by operating constraints: only the RWS and the charge per hole remain adjustable. Switching from ANFO to EXPLUS 90 reduces X50 by nearly 30%, while increasing the charge from 72 to 108 kg at constant RWS reduces it by about 23%; by contrast, the uniformity index n would only improve through a modification of the geometry itself. These results should, however, be read with the caveats inherent to the model, which assumes a unimodal distribution, characterises the explosive using RWS alone without incorporating VOD or detonation pressure — both of which are nonetheless decisive on hard rock — and treats the rock mass as homogeneous, ignoring the detonation sequence. Recalibration using the modified Kuz-Ram model (Gheibie et al., 2009), which notably corrects the underestimation of fines, could be considered in a future study.

The application conditions remain favourable here (hard rock assumed homogeneous, charges between 70 and 110 kg, moderate fracturing), but no post-blast particle size measurement could be carried out, owing to the lack of a drone and image-analysis software. Field observations nonetheless point in the same direction: with the current patterns, mainly based on ANFO, the production of oversize boulders is regularly observed, which is consistent with the predicted rate of 58% of boulders larger than 300 mm, i.e. more than one block in two.

At the conclusion of this work, the proposed optimal pattern (Table 7) retains the existing geometry and combines it with EXPLUS 90, for expected results of X50 = 253 mm, P80 = 486 mm and 28.6% oversize above 400 mm. Three recommendations are made. The first, and most immediate, is to replace the current explosives with EXPLUS 90, the only product meeting both industrial requirements, and applicable without modifying the existing drilling equipment. Its higher purchase cost should be offset by downstream savings, but a detailed economic analysis remains to be carried out to confirm this. The second is to optimise the geometry: by reducing the burden from 3.5 m to 3.0 m, the powder factor would rise to about 0.57 kg/m³ and the rate of boulders larger than 300 mm would fall below 30%, while electronic detonators would improve uniformity. The third is to validate the model through a measurement campaign on a few test blasts (drone-based image analysis), in order to recalibrate the rock factor A and, in the longer term, to explore JKMRC-type variants.

**Table 7. Optimal blast pattern proposed for the Diack quarry.**

| Parameter | Retained value |
|---|---|
| **Explosive** | |
| Main explosive | EXPLUS 90 |
| RWS | 157% (ref. ANFO) |
| VOD | 5,500 m/s |
| Detonation pressure | 17 GPa |
| **Blast pattern geometry** | |
| Bench height (H) | 12.0 m |
| Burden (B) | 3.5 m (3.0 m if optimised) |
| Spacing (Es) | 4.0 m |
| Hole diameter (D) | 102 mm |
| Stemming length (Lb) | 1.5 m |
| Charge per hole | 81.85 kg |
| **Expected results (Kuz-Ram model)** | |
| Median size (X50) | 253.1 mm |
| Percentile 80 (P80) | **486.1 mm ✓** |
| Oversize > 400 mm | **28.6% ✓** |
| Maximum size (P99) | 1,097 mm |

*✓: value meeting the particle size criteria set for feeding the primary crusher. RWS: Relative Weight Strength (ANFO reference = 100); VOD: Velocity of Detonation; X50: median diameter; P80, P99: 80th and 99th percentiles of the particle size distribution.*

## 5. CONCLUSION

This study, carried out by applying the Kuz-Ram model at constant geometry, made it possible to compare four explosives on the hard basalt of Diack and to clearly rank their performance. It shows that EXPLUS 90 constitutes the optimal solution: it is the only explosive to simultaneously achieve a P80 below 500 mm and an oversize rate below 30%, and it can be adopted without modifying the current equipment. The study also highlights an important point: the absolute charge per hole can outweigh the relative weight strength of the explosive.

These results remain predictions from an empirical model and will need to be confirmed by field measurements. The approach followed nonetheless remains reproducible and could be adapted to other quarries facing the same fragmentation difficulties.

### *Declaration by Authors*

**Acknowledgement:** The author thanks the Technical Direction of EPC MINEEX for access to the blast records and rock mass characterisation data for Diack, and ENSMG (UCAD) for the scientific framework of this study.

**Source of Funding:** None

**Conflict of Interest:** No conflicts of interest declared.



## REFERENCES

1. Bellion, Y., Guiraud, R., 1984. Le bassin sédimentaire du Sénégal : synthèse des connaissances actuelles [in French]. BRGM & Direction des Mines et de la Géologie, Dakar.
2. Cantagrel, J.-M., Lappartient, J.-R., Tessier, F., 1976. Nouvelles données géochronologiques sur le volcanisme ouest-africain. *4ème Réunion Annuelle des Sciences de la Terre*, Paris, p. 93
3. Crevola, G., Cantagrel, J.-M., Moreau, C., 1994. Le volcanisme cénozoïque de la presqu'île du Cap-Vert (Sénégal): cadre chronologique et géodynamique. Bulletin de la Société Géologique de France 165 (5), 437–446.

4. Cunningham, C.V.B., 1983. The Kuz-Ram model for prediction of fragmentation from blasting. In: Holmberg, R., Rustan, A. (Eds.), Proceedings of the 1st International Symposium on Rock Fragmentation by Blasting. Luleå University of Technology, Luleå, pp. 439–453.
5. Cunningham, C.V.B., 1987. Fragmentation estimations and the Kuz-Ram model – four years on. In: Fourney, W.L., Dick, R.D. (Eds.), Proceedings of the 2nd International Symposium on Rock Fragmentation by Blasting. Society for Experimental Mechanics, Keystone, pp. 475–487.
6. Cunningham, C.V.B., 2005. The Kuz-Ram fragmentation model – 20 years on. In: Holmberg, R. (Ed.), Brighton Conference Proceedings. European Federation of Explosives Engineers, Brighton, pp. 201–210.
7. Dia, A., 1980. Contribution à l'étude des caractéristiques pétrographiques, pétrochimiques et géotechniques des granulats basaltiques de la presqu'île du Cap-Vert et du plateau de Thiès (carrière de Diack, Sénégal) [in French]. Ph.D. thesis, Université de Dakar, Faculté des Sciences et Techniques.
8. Djordjevic, N., 1999. A two-component model of blast fragmentation. In: Proceedings of the 6th International Symposium on Rock Fragmentation by Blasting. SAIMM, Johannesburg, pp. 213–219.
9. EPC Groupe, 2014. Caractérisation géologique et géomécanique des massifs rocheux pour l'abattage à l'explosif. EPC Groupe, Paris.
10. EPC Groupe, 2017. Maîtrise du minage: conception et réalisation de plans de tir [in French]. EPC Groupe, Paris.
11. Fraudet, P., 1970. Contribution à l'étude des roches éruptives de la région de Thiès (Sénégal) [in French]. Thesis, Université de Lyon.
12. Gheibie, S., Aghababaei, H., Hoseinie, S.H., Pourrahimian, Y., 2009. Modified Kuz-Ram fragmentation model and its use at the Sungun Copper Mine. International Journal of Rock Mechanics and Mining Sciences 46 (6), 967–973.
13. Houssam, B., 2020. Optimisation des paramètres de tir et choix du plan de tir (conditions de la S.N.C. ZITI & ISAADI, Sétif) [in French]. Master's thesis, Université de Béjaïa.
14. Kuznetsov, V.M., 1973. The mean diameter of the fragments formed by blasting of rock. Soviet Mining Science 9 (2), 144–148.
15. Liger, J.-L., 1980. Structure profonde du bassin côtier sénégalo-mauritanien: interprétation de données gravimétriques et magnétiques. Thesis, Université d'Aix-Marseille.
16. Ndiaye, M. (2012). Etude sismostratigraphique et sédimentologique du Bassin Sénégalo-mauritanien dans le secteur de Diourbel et Thiès. Thèse de doctorat, no. Sc. 4445, Univ. Genève.
17. Niane, O., 2011. Étude des vibrations et de la surpression générées par les tirs de mine de la carrière de Bargny (SOCOCIM Industries). Engineering thesis, ENSMG, Dakar.
18. Ouchterlony, F., 2005. The Swebrec function: linking fragmentation by blasting and crushing. Mining Technology 114 (1), 29–44.
19. Ouchterlony, F., Sanchidrián, J.A., 2019. A review of development of better prediction equations for blast fragmentation. Journal of Rock Mechanics and Geotechnical Engineering 11 (5), 1094–1109.
20. Ponsard, J.-F., 1988. The Pan-African orogenic belt of the southern Mauritanides and northern Rokelides. Journal of African Earth Sciences 7 (5-6), 821–828.
21. Protodyakonov, M.M., 1926. Classification des roches selon leur dureté en minage [in Russian]. Academy of Sciences of the USSR, Moscow.
22. Roger, J., Barusseau, J.-P., Castaigne, P., Duvail, C., Noël, B.J., Nehlig, P., Serrano, O., 2009. Notice explicative des cartes géologiques à l'échelle 1/200 000 du bassin sédimentaire sénégalais (Projet PASMI). Direction des Mines et de la Géologie, Dakar.
23. Rosin, P., Rammler, E., 1933. The laws governing the fineness of powdered coal. Journal of the Institute of Fuel 7, 29–36.
24. Sene, S., 2011. Caractérisation géologique de la carrière de Xewell Cimenteries: plan d'exploitation et optimisation des tirs de mine. Engineering thesis, ENSMG, Dakar.
25. Spengler, A. de, Castelain, J., Cauvin, J., Leroy, M., 1966. Le bassin secondaire et tertiaire du Sénégal [in French]. Association

des Services Géologiques Africains, New Delhi.
26. Tessier, F., 1952. Contributions à la Stratigraphie et à la Paléontologie de la Partie Ouest du Sénégal," Thèse Université de Marseille, et Bulletin de la Direction des Mines et de la Géologie de l'Afrique Occidentale Francaise, tome 2, No. 14, 1952, 544 p.

How to cite this article: Moumar DIEYE, Ablaye THIAM, Abdoul Aziz NDIAYE, Rokhaya Sall MBAYE, Souleye SENE. Blast fragmentation prediction and explosive selection using the Kuz-Ram model: the case of the Diack basalt quarry (Senegal). *International Journal of Research and Review*. 2026; 13(9): 123-134. DOI: *https://doi.org/10.52403/ijrr.20260914*

******